Dual transcriptomics and proteomics analyses of the early stage of interaction between Caballeronia mineralivorans PML1(12) and mineral

Stephane Uroz, Laura Picard, Marie-Pierre M.-P. Turpault, Lucas Auer, J. Armengaud, P. Oger

Dual transcriptomics and proteomics analyses of the early stage of interaction between *Caballeronia mineralivorans* PML1(12) and mineral

AUTHORS: Uroz, S. [1,2*], Picard, L.[1,2], Turpault, M-P. [2], Auer L.[1], Armengaud, J.[3], Oger, P.[4]

[1] Université de Lorraine, INRAE, UMR1136 « Interactions Arbres-Microorganismes », F-54280 Champenoux, France

[2] INRAE, UR1138 « Biogéochimie des écosystèmes forestiers », F-54280 Champenoux, France

[3] Université Paris Saclay, CEA, INRAE, Département Médicaments et Technologies pour la Santé (DMTS), SPI, 30200 Bagnols-sur-Cèze, FRANCE

[4] Université Lyon, INSA de Lyon, CNRS UMR 5240, F-69622 Villeurbanne, France

Key words: mineral weathering, *Caballeronia mineralivorans*, transcriptomics, proteomics, geochemistry

*** Corresponding author:** Mailing address:
Université de Lorraine, INRAE, "Interactions Arbres Microorganismes", UMR 1136, 54280 Champenoux, France. Phone: +33 (0)3 83 39 40 81, Fax: +33 (0)3 83 39 40 69. E-mail: stephane.uroz@inra.fr.

ABSTRACT

Minerals and rocks represent essential reservoirs of nutritive elements for the long-lasting functioning of forest ecosystems developed on nutrient-poor soils. While the presence of effective mineral weathering bacteria was evidenced in the rhizosphere of different plants, the molecular mechanisms involved remain uncharacterized. To fill this gap, we combined transcriptomic, proteomics, geo-chemical and physiological analyses to decipher the potential molecular mechanisms explaining the mineral weathering effectiveness of strain PML1(12) of *Caballeronia mineralivorans*. Considering the early-stage of the interaction between mineral and bacteria, we identified the genes and proteins differentially expressed when: i) the environment is depleted of certain essential nutrients (*i.e*., Mg and Fe), ii) a mineral is added and iii) the carbon source (*i.e*., glucose vs. mannitol) differs. The integration of these data demonstrate that strain PML1(12) is capable of i) mobilizing iron through the production of a NRPS-independent siderophore, ii) inducing chemotaxis and motility in response to nutrient availability and iii) strongly acidifying its environment in the presence of glucose using a suite of GMC oxidoreductases to weather mineral. These results provide new insights into the molecular mechanisms involved in mineral weathering and their regulation, and highlight the complex sequence of events triggered by bacteria to weather minerals.

Originality-Significance Statement

The access and the recycling of nutrients are key processes in nutrient poor environments. In such environments, plants have developed particular strategies to adapt, notably based on the selection in their rhizosphere of functional communities effective at collecting the nutrients available in the soil or at weathering minerals. Bacteria are considered as very effective at weathering, but our understanding of the molecular mechanisms, the genes and potential regulations involved during the mineral-bacteria interaction and the mineral weathering (MW) process remains limited. To date, a comprehensive investigation of MW was performed on only a single model bacterial species, *i.e.* strain CH34 of *Cupriavidus metallidurans*. In this context, we investigated the molecular mechanism regulated in strain PML1(12) of *Caballeronia mineralivorans* (an effective MW bacterial strain) depending on the level of nutrient availability, on the presence of a mineral

and on the carbon source. The novel results obtained through the combination of geo-chemical analyses associated to genomic, transcriptomics and proteomics provided a detailed and comprehensive analysis of the functions activated or repressed depending on the presence/absence of the mineral. Our findings provide relevant information for different field of research such as environmental genomics, geochemistry, mineralogy and soil sciences.

Introduction

Minerals and rocks represent an essential source of inorganic nutrients for the long lasting functioning of nutrient-poor or/and low-input ecosystems (April and Newton, 1992). Indeed, beside the nutrients originating from organic matter decomposition and atmospheric deposits, they are the main reservoirs of nutritive elements such as magnesium, potassium, calcium and iron. However, the nutritive content of these minerals remains entrapped into their crystal structure and is not directly accessible to the biosphere. Beside their nutritive role, minerals and rocks also serve as physical supports for the attachment and the development of complex microbial communities (Hutchens *et al*., 2009; Or et al., 2007). They can consequently be considered as reactive interfaces where inorganic nutrients are released and a microbial habitat (*i.e*., the mineralosphere) (Uroz *et al*., 2015). The dissolution of these minerals (*i.e*., mineral weathering) is known to depend on the physico-chemical properties of these minerals (Brantley *et al.*, 2008), the action of abiotic processes (protons, water circulation), and to be amplified through the action of plants, fungi or bacteria (Drever, 1994; Landeweert *et al*., 2001). However, our understanding of the linkage between minerals, microorganisms and nutrient availability and the impact of these factors on mineral weathering remains limited. From the few studies that have analyzed the mineral-colonizing bacterial communities into the soil, it seems that this colonization depends on the weatherability of the minerals, their nutritive content but also the local nutrient availability (Colin *et al*., 2017; Hutchens *et al*., 2009; Vieira *et al*., 2020).

Resource availability is known to affect the structure of the bacterial communities. While for certain categories of substrates (*e.g*., carbon and nitrogen related), the presence of the substrate allows for the enrichment of substrate-degraders, for other substrates (*e.g*., iron) the low concentrations, or depletion, of the substrates allow for the selection of oligotrophic microorganisms capable of recovering this substrate from its insoluble forms or of using alternative substrates. It seems to be the case for mineral weathering bacteria (Huang *et al*., 2014; Wang *et al*., 2014; Uroz *et al*., 2009). Indeed, it has been shown through direct observation or after fertilizations that this functional ability is enriched in nutrient depleted conditions. Such relation was reported for grassland or forest ecosystems, where an enrichment of effective mineral weathering bacteria was observed in soils presenting the lower availability of P and/or the lower nutrient availability compared to nutrient-rich soils (Mander *et al*., 2016; Nicolitch *et al*., 2016). Similarly, several studies analyzing different horizons of a soil profile revealed an

enrichment of mineral weathering bacteria in the deeper and nutrient-poorer horizons (Huang *et al*., 2014; Wang *et al*., 2014). Fertilization with calcium, potassium and/or magnesium was also shown to affect the structure of the mineral weathering bacterial communities (Uroz *et al*., 2011; Lepleux *et al*., 2012; Nicolitch *et al*., 2019). In this case, the amended conditions presented a lower frequency of effective mineral weathering bacteria compared to the non-amended treatment. These findings were confirmed through short-term microcosm experiments, where a single input of Mg or K in a nutrient-poor soil was shown to quickly (*i.e*., 15 days) modify the frequency and effectiveness of mineral weathering bacteria (Nicolitch *et al*., 2019). Together, these studies suggest that the mineral weathering bacterial communities are reactive to variations of nutrient availability, making them especially competitive in nutrient-poor conditions.

At the cell level, nutrient limitation is known to induce important physiological regulations in bacteria, notably increasing the production of secondary metabolites, the expression of uptake systems and in certain cases motility and chemotaxis (Andrew *et al*., 2003; Buch *et al*., 2008; Childers *et al*., 2002 ; Ishige *et al*., 2003 ; Zheng *et al*., 2017). These modifications evidence the capability of bacteria to perceive environmental changes and to adapt to them. One of the best documented example is when iron is depleted in their environment (Cai *et al*., 2018; Lim *et al*., 2012; Sasnow *et al*., 2016). In such conditions, bacteria activate the production of iron chelating molecules (*i.e*., siderophores, haem) and enzymes (*i.e*., deferrochelatase, haem oxygenase) involved in the access to iron as well as the expression of dedicated transport systems (i.e., TonB dependent or ABC transporters/permeases) (Andrew *et al*., 2003; Lim *et al*., 2012). Due to their high affinity with ferric iron and the presence of this microelement in several types of minerals, the production of siderophores has been proposed as one of the main molecular mechanism used by bacteria to weather minerals (Ahmed *et al*., 2014 ; Liermann *et al*., 2000). Indeed, these molecules may directly recover the iron entrapped into the minerals or indirectly by changing the equilibrium of the solution chemistry through the chelation of the available iron. Phosphorous represents another important nutrient, which is frequently found limiting in soils. In P depleted conditions bacteria have been shown to regulate a wide array of genes (Ishige *et al*., 2003; Zeng *et al*., 2016, 2017). Glucose metabolism, ABC transporters and Pho system are generally down-regulated under P depleted conditions (Zheng *et al*., 2016; 2017). Notably, the expression of a pyrroloquinoline quinone (PQQ)-glucose dehydrogenase gene, an enzyme involved in the solubilization of inorganic phosphorous (Goldstein, 1995), was shown to decrease in

Pseudomonas when the concentration of soluble phosphate increased in solution (Zheng *et al*., 2016). The important changes occurring in depleted conditions and the modulation of the production of chelating and/or acidifying molecules suggest that bacteria may have developed molecular mechanisms suitable to interact and to recover the nutrients entrapped into the minerals, but experimental demonstrations are missing.

Comparatively to the studies deciphering the physiological responses of aerobic bacteria to depleted vs repleted conditions, their physiological responses to the presence of a mineral remains under-investigated. To our knowledge, the sole work addressing this question and providing a comprehensive view was done on strain CH34 of *Cupriavidus metallidurans*, an organism isolated from Icelandic basalt (Olsson-Francis *et al*., 2010; Bryce *et al*., 2016). Using whole-genome microarray and proteomics, the authors revealed that this bacterial strain up-regulated the expression of genes, or produced higher levels of proteins, involved in phosphate uptake, nutrient transport, metal and redox homeostasis and motility in presence of basalt, while TonB-dependent transporters and siderophore production appeared down-regulated (Olsson-Francis *et al*., 2010; Bryce *et al*., 2016). In addition, Xia *et al*. (2012) evidenced the up-regulated production of some proteins (assigned as glycine hydroxyl-methyltransferase, phosphoserine aminotransferase, and ketol-acid reducto-isomerase) in a strain of *Bacillus mucilaginosus* in presence of a K- bearing mineral (*i.e*., feldspar). Those first results suggest that complex mechanisms are activated or repressed during the mineral-bacteria interaction, but our knowledge remains limited to few bacterial strains and experimental conditions.

In this context, we investigated the molecular mechanisms used by strain PML1(12) of *Caballeronia mineralivorans* to interact with and weather minerals. This strain was isolated from a nutrient-poor forest soil and was previously characterized for its high mineral weathering effectiveness (Uroz *et al*., 2007) and its ability to promote tree growth (Calvaruso *et al.*, 2006, 2013 ; Koele *et al*., 2009). In this study, we developed a microcosm approach to investigate i) the genes and proteins regulated in condition of deficiency of certain nutritive elements, ii) the genes and proteins regulated in presence of a mineral in such depleted conditions and iii) how the carbon source (*i.e*. glucose vs. mannitol) impacts the response of strain PML1(12). To answer these questions, we used a dual transcriptomics and proteomics approach combined with solution and mineral chemistry to document the physiological processes activated or repressed at the early stage of the interaction between mineral and bacteria.

RESULTS

Chemical analyses of the solution

The analyses done on the solution after 20h of incubation (*i.e.*, culture medium) revealed significant differences between the different treatments (GB, Glucose with bacteria; GBwB, glucose with bacteria and biotite; MBwB, mannitol with bacteria and biotite) (Table 1; Figure 1). The measures done on the abiotic controls (C, Control without bacteria and biotite and CB, Control with biotite without bacteria) confirmed that in the absence of biotite, the culture medium was depleted in iron and magnesium ($p<0.05$). The addition of biotite modified the solution chemistry, provoking a significant increase in solution of the nutrients originating from biotite dissolution. The spontaneous hydrolysis of minerals when introduced in aqueous solution is well-described phenomenon, especially for mineral particles freshly prepared (Brantley, 2008). Due to the spontaneous hydrolysis of biotite, the amount of iron, aluminium and magnesium were increased ($p<0.05$), making the medium amended with biotite capable of sustaining all the nutritional needs of strain PML1(12).

In absence of biotite, the inoculation of PML1(12) (*i.e.*, GB treatment) lead to the same solution chemistry as the non-inoculated treatment (*i.e.,* C treatment), except that the pH of the solution decreased from pH 6.5 to 2.78. The comparison of the treatments amended with biotite and containing glucose evidenced a significant increase of the copncentration of iron, magnesium and aluminium in the solution of the inoculated treatment, while the concentrations of other nutrients (Na, P, Ca) decreased ($p<0.05$). In presence of glucose (GB and GBwB), the pH of the solution reached a value of 2.77 in presence or absence of biotite. When the microcosms were amended with mannitol (MBwB) as carbon substrate only a significant increase of the concentration of aluminium in the solution of the inoculated treatment and a decrease of Na and P were observed, without variations of the concentrations of magnesium and iron in comparison to the control. In presence of mannitol, the pH of the solution reached a value of 4.03. Last, the comparison of the treatments amended with biotite and a carbon source (i.e., glucose (GBwB) or mannitol (MBwB)) evidenced a significant increase of the concentration of iron, magnesium and aluminium in the solution of the glucose amended treatment (GBwB ; $p<0.05$), and no

189 differences for the other nutrients (Na, P, Ca). The pH of the solution appeared significantly more
190 acidic in the treatment amended with glucose than with mannitol ($p<0.05$).
191 In the inoculated treatments, the main organic acids detected were gluconate and pyruvate
192 (Figure 1). Very low concentrations of lactate, formate, oxalate and acetate were detected. In
193 presence of glucose, significantly more gluconate was produced in absence (GB, 874 mg L^{-1})
194 than in presence of biotite (GBwB, 586 mg/L; $p<0.05$). Gluconate concentration was
195 comparatively very low in presence of mannitol (3.65 mg L^{-1}). No organic acid was detected in
196 the abiotic treatments.
197
198 *Physiological properties*
199 When the growth assays were done in the presence of iron and magnesium, no difference was
200 observed in the first 20h of incubation between the glucose or mannitol conditions (Figure S1).
201 However, we observed that for longer incubation periods, a higher biomass was obtained with
202 mannitol (OD_{max}=0.8 after 46h ; ca. 8.10^8 cell mL^{-1}) compared to glucose (OD_{max}=0.65 after 40h;
203 ca. 5.10^7 cell mL^{-1}). In the absence of iron, we observed a delay in growth in comparison to the
204 nutrient rich (*i.e.*, with iron and magnesium) conditions, but no significant difference in the first
205 20h of growth between the glucose and mannitol conditions. In such environments, a higher
206 biomass was obtained with mannitol (OD_{max}=0.53 after 65h; ca. 3.10^7 cell mL^{-1}) compared to
207 glucose (OD_{max}=0.47 after 55h; ca. 8.10^6 cell mL^{-1}) (Figure S1). In absence of iron in the culture
208 medium, the chromazurol assay highlighted that strain PML1(12) produced a chelating agent in
209 both glucose and mannitol treatments (Figure S2). In presence of iron, no chelating agent was
210 detected using the CAS assay. Similarly, no chelating agent was detected in the culture
211 supernatant in presence of biotite.
212
213 *Transcriptome and proteome statistics and comparisons*
214 After 20h of incubation, the same samples were used to extract RNA and recover proteins. For
215 the RNAseq dataset, the number of reads retained after barcode removal and quality control,
216 varied from 35 to 45 million, giving a total of 138 Gb of 150bp paired-end sequence data.
217 Between 98.16 and 99.78% of reads mapped at least once on the genome of *C. mineralivorans*
218 PML1(12). After the removal unmapped sequences and the remaining rRNA sequences, between
219 80 to 91% of the total number of reads were retained. Without log2Foldchange (log2FC)

threshold, a total of 3,984 and 3,644 differentially expressed genes (DEG); corresponding to 43.5 and 39.8% of the genes of PML1(12), respectively) were detected in GBwB and MBwB treatments with a significant pvalue (details in material and methods). When a threshold of 1/-1 (log2FC) was applied, DEG numbers reached 1,153 and 1,241 (corresponding to 12.6 and 13.5% of the genes of PML1(12), respectively) in the GB/GBwB and GBwB/MBwB treatment comparisons respectively. The proteomics dataset consisted in a total of 576,330 MS/MS spectra that were recorded at high resolution, among which 368,661 (61%) were assigned to peptide sequences attributed to strain PML1(12). The number of peptide sequences per sample varied from 25,000 to 37,000. Based on stringent parameters (at least two peptides per protein and FDR below 1%), a total of 2,408 proteins were identified.

To obtain a global view of our dataset, multivariate analyses (*i.e.,* Partial Least Squares regression (PLS)) was performed. Due to the high amount of genes and to permit a good and interpretable visualization of the genes associated to each treatment a Sparse Partial Least Squares regression (sPLS) was preferred to a PLS analysis. These analyses clearly permitted to visualize the differentiation of the treatments (*i.e.*, GB vs GBwB vs MBwB). Both the RNA-based, the protein-based and the combined (RNA+protein) analyses gave a good separation of the different treatments considered (Figure 2). The list of the genes the most associated to each treatment whatever the approach (i.e., RNA or protein) is presented in Table S1. This global analysis was then completed by a detailed analysis using DESeq2. For each treatment comparison (*i.e.*, GB vs GBwB or MBwB vs GBwB), the transcriptome and proteome data were compared according to the differential expression/abundance (i.e., RNA and proteins). These analyses revealed that though the proteomes were supported by a smaller number of proteins identified as significantly differentially produced (DPP) compared the DEG of the transcriptomes, the sequences encoding these proteins were found in the related transcriptome. In the comparison GB/GBwB, 100% of the differentially produced proteins (i.e., 41 in total) were recovered in the 1153 DEG of the related transcriptome (Figure 3A). In the comparison GBwB/MBwB, 82% of the DPP (*i.e.*, 198 in total) were recovered in the 1241 DEG of the related transcriptome (Figure 3B). The comparison of the DEG and DPP obtained through the transcriptomic and proteomics approaches revealed significant correlations according to linear regression analyses ($p<0.0001$; R^2: 0.78 for GB/GBwB; R^2:0.58 for GBwB/MBwB), showing that the common down- and up-regulated genes followed the same trend in the transcriptome and proteome datasets. The genes

differentially regulated (|log2FC|≥1) and common to the RNAseq and proteomics dataset are presented in Table 2.

Overview of the variations in the Clusters of Orthologous Groups (COG)

Although the depth of analysis was very different between the two methods (i.e., proteomics and transcriptomics), a functional analysis was performed to assign the differentially regulated genes of *C. mineralivorans* PML1(12) into the COG categories both at the RNA and protein levels (Figure 4). In the glucose treatments (*i.e.*, GB vs GBwB), the higher percentages of DEG and DPP were observed for the amino acid transport and metabolism (RNA: 11.2% vs Protein: 17 %), cell wall/membrane/envelope biogenesis (RNA: 8.2% vs Protein: 19.5 %), carbohydrate transport (RNA: 8.2% vs Protein: 19.5 %) and inorganic ion transport and metabolism (RNA: 7.45% vs Protein: 19.5 %). The main differences between these two treatments in the transcriptome were observed for cell motility (6% in GBwB vs 0.13% in GB), cell wall/membrane/envelope biogenesis (6% in GBwB vs 2.2% in GB) and in carbohydrate metabolism and signal transduction (Figure 4AB). A focus on the GB treatment revealed only a higher proportion of DEG in the categories S (poorly characterized functions, GB:3.85 % vs GBwB:1.72%), H (coenzyme transport and metabolism, GB:1.40 % vs GBwB:0.66%) and K (Transcription, GB:3.36 % vs GBwB:2.78%) detected by the transcriptome. At the proteome level, several COG categories were not detected in the GB treatment among the DPP (*i.e.*, C,D,F,G,H,K,L,N,S). Cell wall/membrane/envelope biogenesis and amino acids were more represented in the GBwB treatment, while only the category P (Inorganic ion transport and metabolism) appeared higher in the GB treatment (GB: 12.20% vs GBwB:4.88%).

In the comparison glucose (GBwB)/mannitol(MBwB) treatments, the higher proportions of DEG/DPP were observed for amino acid transport and metabolism (RNA: 21.5% vs Protein: 16.7 %), cell wall biogenesis (RNA: 8% vs Protein: 10 %), carbohydrate transport (RNA: 8.6% vs Protein: 13.6 %), signal transduction (RNA: 7.2% vs Protein: 11 %) and inorganic ion transport and metabolism (RNA: 7.5% vs Protein: 3.5 %)(Figure 4CD). Most of the categories were mainly found in the MBwB treatment, except the categories C, D, H and O. The same distribution was observed in the proteome.

Functional changes induced by growth in nutrient-deprived conditions

The comparison done between the GB and GBwB treatments permitted to identify the genes and/or proteins significantly expressed in the condition deprived in iron and magnesium. On the 1,153 DEG and the 41 DPP identified in the comparison of the GB/GBwB treatments, a total of 621 and 23 were significantly higher in the GB treatment in the transcriptome and proteome, respectively.

Among the most up-regulated genes or the proteins presenting an increased abundance in the GB treatment (Table S2A and B), several appeared involved in ion transport. Indeed, higher signal were observed for ion porin (KLU25682.1; log2FC:5.5) or transporter (KLU24497.1), ion permease (KLU25664.1; Log2FC:5.5). All these genes are homologous to genes coding for proteins predicted to allow the incorporation of manganese, magnesium, potassium or phosphorous. Interestingly, the molecular markers supporting these functions were members of the top 5 of the up-regulated genes in the DEG dataset and the most produced in the DPP dataset.

A total of 33 genes involved in iron access and storage appeared up-regulated in the nutrient-deprived condition (*i.e.*, GB). Several iron transporter/receptors (TonB and ABC types) were in the top 20 of the most expressed genes (Table S2A and B). Indeed, 5 of the 20 putative TonB receptors detected in the genome of PML1(12) were significantly up-regulated. In addition, a cluster of 9 successive genes (KLU26370.1 to KLU26361.1) encoding a putative siderophore was detected using antiSMASH based on the presence of the gene KLU26365.1 (log2FC:4.4) presenting high homology to the *IucA/IucC* system, know in *Escherichia coli* to code for the production of aerobactin. In addition, two regions involved in the mobilization of iron from the cell reserve appeared significantly more expressed. The first region is composed of a gene encoding a putative deferrochelatase (KLU25830.1, log2FC:4.5) and several neighbouring genes (KLU25828.1-KLU25831.1) appeared up-regulated. The second region (KLU20274.1-KLU20238.1) is characterized by the presence of a bacterioferritin-associated ferredoxin, iron transporters and a permease, all up-regulated. Several of the proteins specified by these genes were also recovered in the proteins presenting an increased abundance in the comparative proteome analysis as for example the deferrochelatase (KLU25830.1), iron ABC transporter (KLU25829.1, KLU25827.1) (Table S2A and B).

Different genes related to glycogen, glucose and by-product metabolisms appeared up-regulated according to the transcriptome data. Notably, several genes encoding enzymes involved in the synthesis of glycogen and trehalose were detected (Glycogen operon protein homologous

to GlgX (KLU21704.1, log2FC:2.6) ;Glycogen debranching enzyme (KLU25338.1, log2FC:1.5); Glycogen synthase (KLU25341.1, log2FC:2.1) ; trehalose-6-phosphate synthase (KLU22111.1; log2FC:1.8); Malto-oligosyltrehalose synthase (KLU25336.1, log2FC:2.4) ; Trehalose synthase (KLU25392.1, log2FC:2). Among the genes related to glucose metabolism, two regions involved in the production of gluconic acid were detected among the up-regulated genes. The first region corresponds to the locus encoding a flavin adenine dinucleotide (FAD)-dependent enzyme presenting high sequence similarity with a Glucose/methanol/choline (GMC) oxidoreductase. This enzyme (termed GMC1) is composed of three subunits, a large unit (KLU25169.1, log2FC:1.1), a small unit (KLU25168.1, log2FC:1) and a cytochrome unit (KLU25978.1, log2FC:1.1), all the corresponding cistrons being significantly up-regulated. The second region encompasses genes coding for proteins involved in the synthesis of pyrroloquinoline quinone (pqq), which is known to be the cofactor of pqq-dependent enzymes such as the glucose dehydrogenase. Based on sequence similarity, genes *pqqA*, *B*, *C*, *D*, *E* as well as several pqq-dependent enzymes were detected in the genome of the strain PML1(12). Three of the pqq-dependent enzymes have as potential substrates methanol (*i.e.*, pqq-dependent methanol DH; KLU21389.1 and KLU25669.1) and glucose (pqq-dependent glucose DH; KLU26637.1), while the substrate for the last one remains undefined (pqq-dependent alcohol DH ; KLU25853.1). Among the cofactor genes, *pqqB*,*C*,*D* and *E* (1.2 <log2FC<1.6) were up-regulated in the GB treatment, with a low expression level. For the pqq-dependent enzymes, all were expressed, but only genes KLU25853.1 (Log2FC:1.3), KLU25669.1 (Log2FC:0.9) and KLU21389.1 (Log2FC:0.6) were slightly up-regulated, but poorly expressed. In addition, gene KLU20907.1 encoding a 2,5-diketo-D-gluconic acid reductase (i.e., the enzyme which catalyzes the reduction of 2,5-diketo-D-gluconic acid to 2-keto-L-gulonic acid) appeared significantly up-regulated (Log2FC:2.2) in the nutrient limited treatment.

Changes induced by growth in nutrient-deprived condition amended with biotite

The comparison done between the GBwB and GB treatments permitted to identify the genes and/or proteins significantly expressed in presence of biotite. However, biotite spontaneously releases nutrients in the medium as observed by comparing the CB and GBwB treatments at the chemical level (Table 1). Consequently, part of the transcriptomics and proteomics changes observed correspond to a sum of mechanisms involved in the perception and adaptation to the

presence of the mineral, but also to the different nutrients released in the solution from the biotite (part from the spontaneous dissolution and part related to the mineral weathering ability of strain PML1(12)). Among the DEG and DPP identified molecular players, 532 and 18 were significantly higher in the GBwB treatment (compared to the GB treatment) in the transcriptome and proteome, respectively (Table S3A and B).

A total of 43 genes involved in motility presented a higher expression in presence of the mineral, although no surface adhesion was observed. Notably, 34 genes of a cluster of 38 successive genes (KLU23267.1 to KLU27815.1) are involved in flagella construction and functioning (Table S3A and B). Some of these genes as well as from other genomic regions were present in the top 10 of the most up-regulated genes such as FliS (KLU23268.1, log2FC:4.4), FliT (KLU23267.1, log2FC:4.1), flagellin synthesis (KLU23267.1, log2FC:4.1). Notably, the flagellin synthesis (KLU23267.1) was also found in the proteins presenting an increased abundance (log2FC:2). In addition to the motility, several genes related to chemotaxis or linking chemotaxis/motility (n=24) were up-regulated. It was notably the case of several genes annotated as *cheB*,*D*,*E*,*Y* homologs and grouped in the same genomic region (KLU22901.1 to KLU22934.1). Beside the Che related genes, several genes encoding methyl-accepting chemotaxis sensory transducers (n=16) were also up-regulated.

Different genes related to monosaccharides and byproduct metabolisms appeared up-regulated in presence of the mineral according to the transcriptome data, confirming the analyses done at the COG level. Several genes encoding glycosyl transferases such as (e.g., KLU27900.1, KLU27927.1, KLU27959.1, KLU27926.1, KLU27889.1, KLU20777.1, KLU20776.1, KLU20778.1, KLU26149.1, KLU26333.1, KLU26150.1). Among these genes related to glucose metabolism, a region potentially involved in the production of gluconic acid was detected. It corresponded to a flavin adenine dinucleotide (FAD)-dependent enzyme presenting high sequence similarity with a second GMC oxidoreductase. This enzyme (termed GMC2) is composed of three subunits encoding a large unit (KLU25979.1), a small unit (KLU25980.1) and a cytochrome unit (KLU25978.1), all significantly up-regulated (log2FC:1.1 to 1.9). These genes appeared up-regulated, but expressed at a relatively low level. The GMC2 enzyme presented sequence similarity (21%) with the D-gluconate 2-dehydrogenase large subunit of *Gluconobacter frateurii* (BAH80545.1).

Among the up-regulated genes or proteins, several corresponded to potential reductases involved in the reduction of ammonium (KLU22414.1, log2FC:2.4), sulfate (KLU22416.1, log2FC:2.9) and hydroperoxide (KLU26653.1, log2FC:1.2) and to specific transporters such as gene KLU22692.1 (ammonium transporter, log2FC:3.5).

Change induced by growth in nutrient-deprived condition amended with biotite and according to the carbon substrate

Previous experiments revealed that strain PML1(12) was very effective at weathering biotite in presence of glucose, but poorly effective with mannitol (Uroz et al., 2007). The mineral weathering data presented above confirmed these observations. Both carbon substrates are preferential substrates used by the strain PML1(12) for its growth, with a tendency to grow better with mannitol. To avoid a growth effect and to test the impact of these substrates, a short-term incubation time (20h) was done using mannitol or glucose. The comparison done between the GBwB and MBwB treatments (i.e., presence of biotite but two C substrates) permitted to identify the genes and/or proteins significantly expressed in the condition deprived in iron and magnesium in relation to the carbon substrate available for the growth of strain PML1(12) (Table S4A and B).

The GBwB and MBwB treatment comparison evidenced significant metabolic changes. On the 1241 DEG and the 198 DPP identified in the comparison of the GBwB/MBwB treatments, a total of 370 and 58 were significantly higher in the GBwB treatment in the transcriptome and proteome, respectively. Several genes related to the pentose phosphate, glycolysis, glyoxylate or Entner-Doudoroff pathways appeared significantly more expressed in the GBwB treatment. Among the most up-regulated genes or in the proteins presenting an increased abundance those involved in gluconate and 2-ketogluconate metabolism and transport are noteworthy (KLU20897.1 to KLU20902.1) (Table S4A and B). The genes KLU20902.1 (log2FC:4.8) encoding a putative 2-dehydro-3-deoxygluconokinase and KLU20900.1 (log2FC:4.11) encoding a gluconate-2-dehydrogenase (GADH) were the second and the sixth genes the most up-regulated in the GBwB treatment compared to MBwB, respectively. In addition, several genes encoding GMC oxidoreductases were up-regulated in the transcriptome (GMC1: small (KLU25168.1) / large (KLU25169.1) / cytochrome (KLU25978.1), logFC:1.87 for each subunit ; GMC3: cytochrome (KLU25394.1) / large (KLU25343.1) / small (KLU25394.1), logFC=1.15 for each

subunit), but only the GMC1 (KLU25169.1) presented a significantly increased abundance in the proteome (log2FC:5.49). Several other genes related to cytochrome oxidases involved in the proton motrice force (PMF) and in the electron transport/respiratory chain appeared also up-regulated (Cytochrome d ubiquinol oxidase subunit II, KLU26331.1; Cytochrome b561, KLU25473.1; Cytochrome c-type biogenesis DsbD type, 1.18 RNA and 1.8 protein). Porin and transporters, and efflux systems were also up-regulated (effluxtransporters (KLU24564.1), log2FC:3.54; porin (KLU23737.1), log2FC:3.84). Some genes especially related to the transport and mobilization of iron appeared also up-regulated like some iron permeases (KLU20236.1, log2FC:1.34; KLU25828.1, log2FC:1.08), bacterioferritin (KLU20274.1, log2FC:1.13) and an enzyme involved in the mobilization of iron from the cell (*i.e.*, deferrochelatase/peroxidase EfeN (KLU25830.1, log2FC:1.69).

Comparatively to the GBwB treatment, a higher number of genes and proteins appeared up-regulated in the MBwB treatment (Table S5A and B). Most of these changes were related to mannitol metabolism, which differs from glucose metabolism. Notably several genes encoding mannitol ABC transporter permeases (KLU22511.1, log2FC:5.39; KLU22510.1, log2FC:5.24; KLU22513.1, log2FC:5.01) appeared highly expressed. The gene and protein encoding a mannitol-2-dehydrogenase were significantly up-regulated (KLU22486.1; log2FC:4 with RNA and 3.8 with protein). Notably, the different genes encoding the subunits (KLU25980.1, KLU25979.1, KLU25978.1) of the GMC oxidoreductase (GMC2) appeared up-regulated in the transcriptome in MBwB treatment, but with low expression level and log2FC value of 0.70.

DISCUSSION

To decipher the molecular mechanisms involved in the early stage of the interaction between mineral and bacteria and in the weathering of biotite, we used a combination of transcriptomics, proteomics and (geo)chemistry. The single time-point considered in our study (i.e., 20h) was determined based on preliminary data to be in the early stage of interaction bacteria/mineral/solution at both biological (almost no growth) and mineralogical levels (almost no alteration). Our goal was to obtain a view of the mechanisms activated or repressed without much cell replication and as early as we could quantify biotite dissolution. Indeed, after a longer incubaiton period, cells have the time to replicate differentially between the carbon sources and the system (mineral/solution/bacteria) is no longer deprived in nutrients. The transcriptomics and

proteomics approaches are complementary and provide a more integrative view of the regulated pathways, while the concomitant (geo)chemical analyses tell us about the processes themselves. The RNA-seq approach permitted to identify massively the transcriptional regulatory effects of the different treatments, while proteomics gave access to the most abundant functions activated according to the treatments considered. Although the depth of analysis was very different between the two methods due to the methodologies, it is noteworthy that both provided a congruent view of the molecular basis of mineral weathering. Indeed, we found significant correlations between the proteins differentially produced (PDP) and the genes differentially expressed (DEG) both using DESeq2 and Mixomics analyses. This good overlap is probably linked to the fact that we considered the early stage of interaction between mineral/bacteria (*i.e.*, a short-term event). Our results revealed the pathways activated or repressed in the presence/absence of mineral and according to the available carbon source. Significant changes in the solution chemistry as well as in the transcriptome and proteome of strain PML1(12) were observed, highlighting that as expected strain PML1(12) was reactive to the presence/absence of mineral in its environment and potentially induced molecular mechanisms involved in the mineral weathering process.

The analyses performed on the solution chemistry revealed a stronger acidification in presence of glucose (pH 2.7) than in presence of mannitol (pH 4.03), confirming previous observations on this strain but obtained after a longer incubation time (*i.e.*, 48h; Uroz *et al.*, 2007). In presence/absence of biotite, strain PML1(12) induced the same acidification. In addition, strain PML1(12) was shown to produce a siderophore independently of the carbon source, but dependent on Fe-depletion. The production of siderophore was not detected in presence of biotite, suggesting that the amount of Fe released spontaneously was sufficient to repress its synthesis. The growth assays revealed no difference in biomass development in the first 20h of bacteria/mineral interaction whatever the treatment, evidencing that the differences measured in our setup were not attributable to putative differences in cell growth. After longer incubation times, a growth lag was observed, evidencing the long-term impact of iron and magnesium depletion on the physiology of the bacterial strain. Together with this stronger acidification, we measured a significantly higher dissolution of biotite in the glucose (GBwB) than in the mannitol (MBwB) treatment as revealed by the quantities of iron and magnesium released in the solution. Those results further confirm the strong connection between bacterial metabolism and mineral

467 weathering (Mapelli *et al*., 2012; Uroz *et al*., 2009). Gluconic acid appeared as the main organic
468 acid detected in presence of glucose as carbon source, while it was almost absent in the mannitol
469 treatment. Notably, significantly higher concentrations of gluconic acid was measured in the
470 treatment without mineral (*i.e*., GB; Fe and Mg depleted) than with mineral (*i.e*., GBwB; Fe and
471 Mg released from biotite). Those results suggest that Mg- and Fe-dependent metabolic
472 regulations occur in strain PML1(12). This is congruent with the results of Sasnow *et al*. (2016)
473 showing that when a *Pseudomonas* strain was grown in Fe-repleted conditions, glucose was
474 mostly converted into biomass and CO_2 (96%), while in Fe-depleted conditions it was mostly
475 converted into gluconate (40%), siderophore (10%), CO_2 (30%) and marginally into biomass
476 (10%). Together our results show that the presence of biotite in the culture medium leads to
477 quantifiable chemical and physiological changes as revealed by the differences in the solution
478 chemistry and the differential production of siderophore and organic acids.
479 Due to the depletion of the culture medium in iron and magnesium, the up-regulation of
480 molecular mechanisms involved in the mobilization of iron was expected. While the ability to
481 weather mineral is well known for strain PML1(12), its ability to produce chelating agents was
482 never investigated at both chemical and genomic levels. Interestingly, the transcriptome and
483 proteome analyses revealed that several genes/proteins involved in iron mobilization and
484 transport were up-regulated in the GB treatment. Beside the different transporters and permeases,
485 two main pathways were identified. The first one corresponded to the mechanisms involved in
486 the access to extra-cellular iron. A cluster of genes encoding a putative siderophore appeared
487 among the most up-regulated genes in the Fe-depleted treatment (GB). The siderophore
488 characteristics of this cluster were confirmed by an antiSMASH analysis on the genome, which
489 revealed the presence of *iucA/iucC* homologs. The *iucA/iucC* genes encode a non-ribosomal
490 peptide synthetase (NRPS)-independent siderophore (NIS) synthetase, which is responsible of the
491 condensation of citrate, or a derivative molecule, with an amine or alcohol group, and last of the
492 displacement of a citryl intermediate (Carroll and Moore, 2018). In PML1(12) the gene found
493 presented high sequence similarity (26.5%) with the N(2)-citryl-N(6)-acetyl-N(6)-hydroxylysine
494 synthase (*iucA*) and the aerobactin synthase (*iucC*) of *E. coli*. NIS synthetases produce non-
495 peptidic siderophores such as aerobactin, rhizobactin or woodybactins (Challis, 2005; Carmichael
496 *et al*., 2019; Lynch *et al*., 2001; de Lorenzo *et al*., 1986; Carroll and Moore, 2018). A similar
497 system was also reported as up-regulated by Olsson-Francis *et al.* (2010) in *Cupriavidus*

metallidurans dtrain CH34 growing in Fe-depleted environment compared to the same condition amended with obsidian. Notably, the exact same gene organization found in PML1(12) was observed in the genome of several strains of *Pseudomonas, Massilia, Rasltonia* or *Sinorhizobium* and in some *Burkholderia sensu largo* (conprising *Burkholderia, Caballeronia* and *Paraburkholderia*). The antiSMASH analysis did not identify other siderophore systems such as non-ribosomal peptide synthetases (NRPS) in the genome of strain PML1(12), suggesting that this gene cluster is the only one involved in the production of a siderophore. The second pathway up-regulated in strain PML1(12) corresponded to mechanisms involved in the re-mobilization of intra-cellular iron (Andrews *et al*., 2003). Indeed, several enzymes involved in the mobilization of iron from the cell reserves such as bacterioferritin-associated thioredoxin and deferrochelatase appeared up-regulated in both transcriptome and proteome datasets. Notably, these enzymes have been described to allow for the storage of this element in bacterioferritin in excess of iron to protect the cell against iron toxicity, and to perform the reverse reaction in nutrient-poor conditions (Andrews *et al*., 2003). Together, these data show that under Fe-depletion, strain PML1(12) activates different molecular mechanisms which may participate in its ability to live in nutrient limited conditions and are potentially involved in the first step of the mineral weathering process.

As the production of gluconic acid appeared significantly more important in absence of biotite in the culture medium, a specific focus was made on the genes and proteins related to glucose metabolism which regulation was increased compared to the GBwB treatment. This survey evidenced two important modifications in the cell functioning. The first was related to the up-regulation of genes involved in carbon storage. Indeed, several genes involved in glycogen and trehalose production were up-regulated in the GB treatment. These two carbohydrates are polymers of glucose produced by bacteria as storage compounds. Glycogen and trehalose are usually produced when carbon is abundant but another nutritive element required for growth is limiting **(**Argüelles, 2000; Preiss and Romeo, 1994). The up-regulation of these genes in our experiments clearly evidences the physiological changes induced by Fe and Mg depletion. The second modification is linked to the production of gluconic acid. From the literature, gluconic acid is usually produced by a glucose deshydrogenase (GDH), which releases protons jointly with the production of the gluconic acid. Glucose is usually oxidized in the periplasm to gluconate and partially further oxidized to 2-ketogluconate (Hanke *et al*., 2013). The PQQ-dependent GDHs are

suspected to be key enzymes involved in mineral weathering (Babu-Khan *et al*., 1955; Golstein *et al*., 1995; Wang *et al*., 2020). The genome of strain PML1(12) contains several enzymes related to GDH, some pyrroloquinoline quinone (PQQ)-dependent and some others non-PQQ dependent. Concerning the PQQ-dependent enzymes, this strain possesses three identified enzymes as well as a suite of *pqq* genes (A to E) encoding the PQQ cofactor. All these genes (except *pqqA*) showed a significant up-regulation in GB than in GBwB, but supported by a low expression level. The potential regulation of the PQQ system was reported for some bacterial strains (An and Moe, 2016; Wang *et al*., 2020), but other studies suggested that it may be a constitutive mechanism (Zheng et al., 2017). Concerning the PQQ-independent enzymes, a total of 4 GMC oxidoreductases were detected in this study in the genome of strain PML1(12). These enzymes depend on FAD as co-factor and allow the production of gluconic acid from glucose. In the depleted treatment (GB), only the GMC1 (small subunit (KLU25168.1); large subunit (KLU25169.1) and cytochrome subunit (KLU25978.1)) appeared significantly up-regulated, supported by a high expression level. In addition, a 2,5-diketo-D-gluconic acid reductase was also significantly up-regulated in the depleted treatment (GB>GBwB). This enzyme is involved in the transformation of 2,5 ketogluconic acid into 2 ketogluconic acid. The ionic chromatographic analyses done in our study did not allow to distinguish between the different forms of gluconic acid produced (*i.e*., gluconic acid, 2 ketogluconic acid, 5 ketogluconic acid, or 2,5 ketogluconic acid) by strain PML1(12). However, we showed that strain PML1(12) is capable of using gluconic acid, 2-ketogluconic acid and 5-ketogluconic acid as carbon sources (2,5 ketogluconic acid was not tested), suggesting that this strain produces the different forms and is capable of metabolizing them. Our genomic analyses suggest that strain PML1(12) is capable of forming gluconic acid through two types of GDH depending on two types of co-factors: PQQ or FAD. However, the GMC oxidoreductase showed a far higher expression level than the PQQ-dependent GDH and differential expression in the depleted condition (*i.e*., GB). The down-regulation of a GMC oxidoreductase was also reported for another strain of *Burkholderia* (*B. multivorans* WS-FJ9) when phosphate concentration increased in the culture medium, but its function was not investigated (Zheng *et al*., 2017). Together, our data suggest that this pathway may be the main one involved in the production of gluconic acid in strain PML1(12) in our experimental conditions.

559 The comparison made between the GB and GBwB treatments highlighted the potential
560 molecular mechanisms activated in presence of biotite both using specific (i.e., RNA or Protein)
561 or combined (i.e., RNA + Protein) analyses on our omic data. The transcriptome analysis of these
562 treatments revealed that 12.6% of the genes were differentially expressed, and half of them (532
563 genes; 5.8%) were up-regulated in presence of the mineral. At the COG level, the stronger
564 differences between the two treatments (GB vs GBwB) were related to cell motility, cell
565 wall/membrane/envelope biogenesis and carbohydrate metabolism and signal transduction,
566 suggesting important physiological changes in strain PML1(12) due to the presence of the
567 mineral. The detailed analyses of the DEG confirmed these observations, with the notable
568 increase of the expression of genes involved in flagellum construction and functioning, but also
569 of the PML1(12) homologous genes of the chemotaxis Che system (*cheA*,*B*,*R*,*W*,*Z*). This system
570 allows bacteria to perceive chemical gradients through methyl-accepting chemotaxis proteins,
571 which then regulate the functioning of the flagellum (Wadhams and Armitage, 2004).
572 Interestingly, a similar increase of the motility and chemotactism gene expression was also
573 reported in the few studies dealing with bacteria (*i.e.*, *Geobacter metallireducens*, *Cupriavidus*
574 *metallidurans*) growing in presence of complex minerals or Fe/Mn oxides (Childers *et al.*, 2002;
575 Olsson-Francis *et al.*, 2010; Bryce *et al.*, 2016). The combined activation of the chemotaxis and
576 motility suggests that PML1(12) can perceive the presence of the mineral and/or of the elements
577 released from its structure and migrates probably to the most nutrient-rich zone (*i.e.*,
578 mineral/solution interface). The question was to determine whether, they form a biofilm on
579 biotite. Cell attachment is known to be determined by several factors such as solution chemistry,
580 pH and quorum sensing communications (Banfield and Nealson, 1997; Yee *et al.*, 2000).
581 However, while the cells are able to migrate to the mineral, our microscopic observations have
582 not evidenced the formation of a PML1(12) biofilm on the biotite particles. In addition, in
583 previous experiments we always observed only a few cells on the mineral surfaces after
584 paraformaldehyde or alcohol fixation, suggesting that this strain does not form biofilms and is
585 only poorly adherent on the biotite particles under our experimental conditions. Consequently,
586 our results suggest that biotite dissolution induced by strain PML1(12) occurs without stable
587 colonization of the mineral surfaces and potentially through covalent interactions or distant
588 mechanisms.

589 The specific focus on the treatments with biotite (GBwB and MBwB) allowed us to uncover
590 the physiological changes induced or repressed as a function of the presence of the mineral with
591 two types of carbon source, and to quantify biotite dissolution. From these analyses, it appears
592 clearly that the acidification due to the production of gluconic acid is one of the main
593 mechanisms used by strain PML1(12) to access the nutrients trapped in the mineral. Indeed,
594 when the acidification is limited as in the MBwB treatment, the quantity of gluconic acid is
595 negligible and the dissolution of biotite very low. The genome analysis of strain PML1(12)
596 revealed the presence of a PQQ system and PQQ-dependent dehydrogenases. Indeed, strain
597 PML1(12) harbours the genes *pqqA*,*B*,*C*,*D* and *E* (KLU25599.1, KLU25560.1-KLU25563.1) and
598 some pqq-dependent DH (KLU25669.1:putative methanol DH; KLU21389.1:glucose DH;
599 KLU25669:methanol/ethanol DH). In addition, 4 potential GMC oxideroreductase genes are
600 distributed in the genome: the GMC1 (KLU25168.1), the GMC2 (KLU25978.1), the GMC3
601 (KLU25394.1) and the GMC4 (KLU26513.1). Three of these GMC oxidoreductases (GMC1-3)
602 are composed of 3 subunits (small, large and cytochrome) and correspond to the classical
603 architecture of such enzyme type (Cavener, 1992; Yamaoka *et al.*, 2008). The last GMC (GMC4)
604 detected in the genome does not present such organization and did not present significant up- or
605 down-regulation in the transcriptome or proteome. The GMC superfamily encompasses a wide
606 variety of FAD-dependent oxidoreductases such as gluconate dehydrogenase (GADH) glucose
607 dehydrogenase (GDH), fructose dehydrogenase (FDH), sorbitol dehydrogenase (SDH) (Sützl *et*
608 *al.*, 2019). The sequence comparison of each subunit with one another in our study revealed that
609 the GMC1 and GMC2 presented a high sequence similarity (65%; positive on 75%), while the
610 GMC3 (KLU25394.1) and GMC4 (KLU26513.1) presented a lower similarity (22% and 26%,
611 respectively only on a fraction of the protein sequence). Although their substrate remains
612 undetermined, part of these GMC enzymes may encode FAD-dependent GDH involved in the
613 production of gluconic acid. In this context, we made a correlation analysis for each FAD- or
614 PQQ-dependent enzyme using the expression data and the chemical analyses done for each
615 replicate and each treatment (Figure 5). These analyses revealed no correlation between the
616 quantity of gluconic acid and the expression level of the *pqq* genes (*pqqB,C,D*) and the related
617 PQQ-dependent DH. Although the GMC2 (gene KLU25978.1 and related subunits) was poorly
618 expressed compared to the other GMC1 and 3, we observed negative correlations with the
619 quantity of gluconic acid. These negative correlations and the fact that the GMC2 was up-

620 regulated in the treatments with low gluconic acid concentrations suggests that it does not encode
621 for a GDH. In this sense, the GMC2 large subunit has a strong sequence similarity with the D-
622 gluconate 2-dehydrogenase large subunit of *Gluconobacter frateurii*. Its up-regulation would
623 explain the low concentrations of gluconic acid detected in the supernatant in presence of biotite.
624 In contrast, significant positive correlations were observed between the quantity of gluconic acid
625 and the expression of the GMC1 (genes KLU25168.1 and related subunits) and the GMC3 (genes
626 KLU25394.1 and related subunits), which were the GMCs up-regulated in the GB and GBwB
627 treatments, respectively. Thus, our results clearly show that the production of gluconic acid in
628 strain PML1(12) is probably not due to the pqq system, but to the GMC1 and 3 oxidoreductases
629 and that the presence of glucose and the nutrient availability (*i.e.*, Fe, Mg) and/or the presence of
630 the biotite, induce a fine tuning of these two GMC enzymes in strain PML1(12). Interestingly, the
631 implication of such enzyme type (*i.e.*, FAD-dependent GDH) in mineral weathering was recently
632 evidenced for collimonads, another representative of the Betaproteobacteria (Picard *et al.*,
633 submitted). This study revealed that though collimonads did not contain pqq related genes in their
634 genome, they produce high amounts of gluconic acid and protons through the action of a GMC
635 oxidoreductase capable of oxidizing glucose to gluconic acid.
636 Based on the integration of our data and that of the literature (Olsson-Francis *et al*., 2010;
637 Bryce *et al*., 2016; Sasnow *et al*., 2016; Zeng *et al.*, 2016), we progressed in our understanding of
638 the sequence of events involved in mineral/bacteria interaction and mineral weathering. Although
639 additional experiments are required to support the different steps (*i.e*., other treatments and
640 kinetic analysis), we propose here a hypothetical functional model of the main mechanisms
641 activated by strain PML1(12) during the early stages of the interaction with the mineral that could
642 pave future experiments (Figure 6). i) The initial stage corresponds to the perception of a nutrient
643 depletion. In such condition, PML1(12) triggers the production of a siderophore, which chelates
644 the iron in solution and scavenges the Fe poorly associated to the mineral surfaces. The activation
645 of the production of siderophore in Fe-depleted conditions was expected, as it is a common
646 mechanism regulated in bacteria according to Fe-availability (Olsson-Francis *et al*., 2010;
647 Sasnow *et al*., 2016). At the same time and only in the presence of glucose, the bacterial strain
648 activates the pentose phosphate, glycolysis, glyoxylate and Entner-Doudoroff pathways resulting
649 in the production of gluconic acid and the acidification of the solution (Sasnow *et al*., 2016; Zeng
650 *et al.*, 2016). Among the enzymes activated in strain PML1(12), we can point out the GMC1,

651 which activity is increased in Fe-depleted conditions. Such metabolic changes were recently
652 quantified using isotope-assisted metabolomics in *Pseudomonas putida* strain KT2440 (Sasnow
653 *et al.*, 2016). Comparing Fe-repleted and -depleted conditions, these authors showed a reduced
654 growth, a better glucose uptake and an important production of gluconic acid under Fe-
655 depletion. ; ii) when the acidification reaches a threshold in presence of mineral, siderophore
656 production is stopped as the protons released allow for a significant dissolution of the mineral and
657 for the release of sufficient levels of iron and other nutrients in the solution. Siderophore
658 production is known to be inhibited when Fe or a Fe-carrying mineral is added in a Fe-depleted
659 solution (Olsson-Francis *et al*., 2010; Sasnow *et al*., 2016). This raises questions about the role
660 played by the siderophore in the mineral weathering process. Indeed, as the release of the
661 nutrients entrapped into the mineral occurs spontaneously in aqueous solution and is amplified by
662 the activity of bacteria, we can wonder under which condition siderophores are produced. Indeed,
663 siderophore production is known to be repressed by minutes amount of iron (*e.g.*, 1mg/L or less)
664 (this study; Sasnow *et al*., 2016); iii) due to the increase of nutrients in solution (*i.e*., spontaneous
665 and microbial-increased dissolution), cells activate motility and chemotaxis and are attracted to
666 the mineral/solution interfaces. Interestingly, the *Cupriavidus metallidurans* strain CH34 was
667 also shown to activate motility and chemotaxis in presence of basalt (Olsson-Francis *et al*., 2010),
668 suggesting that motility and chemotaxis may be common features used by bacteria to interact
669 with and weather minerals; iv) when nutrient availability increases in the solution, strain
670 PML1(12) increases the activity of a second GMC oxidoreductase (GMC3) identified as a FAD-
671 dependent GDH; and last, v) when the availability of glucose decreases, cells consume the
672 glucose derivatives (gluconic acids and derivatives; Sasnow *et al*., 2016) and the production of
673 the GMC oxidoreductases is stopped.
674
675 **CONCLUSION**
676 Using a suite of omic approaches and (geo)chemical analyses, we were able to highlight the
677 significant physiological changes occurring in strain PML1(12) during the early stage of the
678 interaction with minerals. The suite of omics used in our study (*i.e*., genome analysis,
679 transcriptome and proteome), their high complementarity and their integration provides a
680 comprehensive view of the molecular mechanisms activated or repressed by this bacterial strain
681 as a function of the presence or absence of the mineral. Notably, the genes evidenced in the

682 DESeq2 analyses of the transcriptomics or proteomics datasets were also found in the combined
683 RNA and proteins approach (*i.e.*, Mixomics), strengthening by this way our conclusions. Our
684 analyses showed that this bacterial strain is well equipped to survive in nutrient-poor
685 environments. Molecular mechanisms involved in iron chelation (NRPS-independent system) and
686 acidification (different types of GDH) appeared up-regulated, but in a different way depending on
687 the presence/absence of the mineral and the availability of Mg and Fe. Noticeably, our study
688 points out that GMC oxidoreductases play a stronger role in the mineral weathering process in the
689 strain PML1(12) than does the PQQ-dependent GDH. To elucidate the dynamics of the next steps
690 of the mineral weathering pathway proposed in our model will require further experimentation
691 and the verification of the role of the different candidate genes identified.
692
693 **MATERIAL AND METHODS**
694
695 *Bacterial strain and culture media*
696 Strain PML1(12) was used in our study as model organism due to its mineral weathering
697 effectiveness (Calvaruso *et al*., 2006; Uroz *et al*., 2007). Initially described as a *Burkholderia*,
698 genomic and physiological analyses allowed us to assign this strain to a new species of the genus
699 *Caballeronia* named *Caballeronia mineralivorans* (Uroz and Oger, 2015; 2017). In addition,
700 metagenomic analyses highlighted that culturable representatives of this genus are particularly
701 enriched in the rhizosphere of trees as well as on the surfaces of minerals (Lepleux *et al.,* 2012;
702 Colin *et al*., 2017). Strain PML1(12) was grown at 25°C in solid and liquid Luria-Bertani (LB)
703 media as well as in 1/10 diluted Tryptic Soy Agar (TSA) medium (Tryptic Soy Broth from Difco,
704 final concentration : 3 g L^{-1} and agar, 15 g L^{-1}). For the microcosm experiment described below, a
705 modified version of the Bushnell-Haas (BHm; devoid of iron and magnesium) medium was used
706 to create a nutrient deficiency complementary to the nutrients contained in the mineral used (*i.e*.,
707 the biotite; description below). The BHm composition was as follows (g L^{-1}): KCl, 0.020;
708 $NaH_2PO_4 \cdot 2H_2O$, 0.080; $Na_2HPO_4 \cdot 2H_2O$, 0.090; $(NH_4)_2 \cdot SO_4$, 0.065; KNO_3, 0.100; and $CaCl_2$,
709 0.020, buffered at pH 6.5 and supplemented with glucose or mannitol (2 g L^{-1}) as carbon source.
710 Glucose or mannitol were selected because they represent the dominant carbohydrate sources
711 found in forest soil (Jolivet *et al*., 2006; Mederiros *et al*., 2006) and also because strain

712 PML1(12) presented differential mineral weathering effectiveness in relation to these two
713 substrates (Uroz *et al*., 2007).
714
715 *Mineral description and preparation*
716 The mineral chosen was a biotite from Bancroft (Canada). Biotite is a 2:1 phyllosilicate,
717 frequently present in acid soils, which weathers relatively quickly and holds K, Mg, and Fe
718 nutrient elements (which are indispensable for plants). Its chemical composition is 41.01% SiO2,
719 10.9% Al2O3, 2.21% Fe2O3, 10.05% FeO, 0.27% MnO, 18.9% MgO, 0.41% Na2O, 9.46%
720 K2O, 2.28% TiO2, 4.42% F, and 0.08% Zn (Calvaruso *et al*., 2006). Its structural formula is
721 (Si_3Al_1) $(Fe^{3+}_{0.12}\,Fe^{2+}_{0.61}\,Mg_{2.06}\,Mn_{0.02}\,Ti_{0.13})$ and $K_{0.88}\,Na_{0.06}\,O_{10}$ $(OH_{0.98}F_{1.02})$. This composition was
722 determined with inductively coupled plasma–atomic emission spectroscopy (ICP-AES), after
723 alkaline fusion with $LiBO_2$ and dissolution in HNO_3. The biotite crystals were ground, treated
724 ultrasonically (2 min, three times at 100V) to remove the fine particles that electrostatically
725 adhere to the particles, washed three times with distilled water, and then sieved (mesh size 200–
726 400 µm) to obtain size calibrated particles. The particles were then dried before any
727 manipulation. Freshly prepared minerals are known to release weak amount of nutrients when
728 introduced in aqueous solution (Brantley, 2008). This spontaneous hydrolysis is due to the
729 physical preparation of the size-calibrated particles.
730
731 *Bacterial inoculum preparation*
732 The bacterial strain PML1(12) was grown from a -80°C glycerol stock on 1/10 diluted TSA agar
733 medium at 25 °C for 48h. A single colony was used to inoculate 50 mL of LB medium and
734 incubated for 48h in at 25 °C. Ten milliliters of this culture were then collected (8,000 g 15 min
735 at 4°C), washed three times in sterile water and suspended in 5 mL sterile water to obtain a
736 calibrated suspension at OD_{595nm} (optical density) = 1 (ca. 10^9 cell mL^{-1}).
737
738 *Experimental design*
739 The microcosms consisted of 100 mL capped Erlenmeyer flasks filled with 45 mL of sterile BHm
740 medium devoid of Fe and Mg, amended or not with 2 g of autoclaved biotite particles (size: 200-
741 400 µm). To avoid iron contamination, all glassware was washed with 3% HCl and rinsed with
742 deionised water. For each inoculated treatment, 5 mL of bacterial inoculum was added. As a

743 spontaneous hydrolysis of biotite is known to occur in aquaeous solution, non-inoculated
744 microcosms containing culture medium with (control with mineral, CB) and without mineral
745 (control without mineral, C) particles were also included. In these treatments, a volume of 5 mL
746 of sterile water was added. For each condition treatment, four flasks were prepared. Our
747 experimental design was determined to allow a comparison between: i) the GB
748 (glucose+bacteria) treatment vs GBwB (glucose+bacteria+biotite) treatment, where GBwB is our
749 baseline (presence of the mineral and of all the nutrients required for growth); ii) the GBwB
750 (glucose+bacteria+biotite) treatment vs the MBwB (mannitol+bacteria+biotite) treatment, where
751 MBwB is our baseline (absence of mineral weathering). No treatment MB (mannitol+bacteria)
752 was considered as strain PML1(12) is not effective at weathering with mannitol (Uroz *et al*.,
753 2007). No 'non nutrient-limited condition' was included in our experimental design as we were
754 interested only in the direct and indirect effects (*i.e.*, the mineralosphere effect; Uroz *et al.*, 2015)
755 of the introduction of the mineral in our system. Microcosms were incubated at 22 °C with
756 agitation at 140 rpm in an orbital shaker (INFORS/Minitron). The duration of our experiment
757 (*i.e.*, 20h) was determined based on preliminary data to be in the early stage of the interaction
758 bacteria/mineral/solution at both biological (almost no growth) and mineralogical levels (almost
759 no alteration). Our goal was to obtain a view of the mechanisms activated or repressed without
760 much cell replication and as early as we could quantify biotite dissolution. Indeed, after a longer
761 period, cells have the time to replicate differentially between the different carbon sources and the
762 system (Mineral/solution/bacteria) is no longer deprived in nutrients. In addition, in our
763 experimental conditions, strain PML1(12) requires more than 4h to replicate and the acidification
764 of the solution in presence of glucose began evident only after more than 18h in our experimental
765 conditions and is maximum after 48h.
766
767 *Chemical analyses*
768 The supernatant was recovered by centrifugation (10,000 g for 15 min) and filtered at 0.22µm
769 (GHP Acrodisc 25 mm syringe filter ; PALL). A volume of 10 mL was used to determine the
770 concentrations of K, Na, P, Ca, Mg, Fe and Al in the different treatments. The analyses were
771 done by inductively coupled plasma-atomic emission spectrometry (700 Series ICP-OES, Agilent
772 Technologies). The pH was measured with a pH meter (DL70 ES, Mettler). Chemical analyses
773 were performed for all replicates. The culture supernatant was also analyzed to determine the

774 major organic acids released by the bacteria. These analyses were performed on an ion
775 chromatography with conductivity detection (ICS 3000, Dionex Corp.) associated to an analytical
776 column (IonPac® AS 11 HC, Dionex corp.) according to Balland *et al*. (2010). The supernatants
777 were eluted with KOH solutions of varying concentrations (0.9–60 mM) over time (step gradient)
778 with a flow rate of 1.3 mL/min. Synthetic organic acids were used as references (sodium formate,
779 D-gluconic acid, sodium butyrate, pyruvic acid sodium salt, sodium citrate tribasic, sodium
780 oxalate, sodium propionate, sodium acetate, succinic acid disodium salt, DL-malic acid disodium
781 salt, sodium-L-lactate and malonic acid disodium salt).
782
783 *Physiological assays*
784 The growth of strain PML1(12) was monitored in order to determine potential biases of biomass
785 development in presence of glucose or mannitol (2g/L) are sole carbon source. To do so, 10 µl of
786 bacterial inoculum was inoculated in 190 µl of medium (corresponding to 1.10^6 cell/mL) with or
787 without iron and magnesium incubated at 25°C. Iron was added as $FeSO_4$ (2.5 mg/L final
788 concentration) and magnesium as $MgSO_4$ (20 mg/L final concentration). The optical density (OD
789 600 nm) was measured during 4 days every 3h using a TECAN microplate reader to follow the
790 growth and determine its maximum (OD max). Similarly, we assayed the ability of PML1(12) to
791 grow on gluconic acid, 2 ketogluconic acid and 5 ketogluconic acid (2 g/L). To determine the
792 potential production of iron chelating agents by strain PML1(12), a volume of 100 µl of inoculum
793 was introduced in 10 mL of medium with glucose or mannitol as sole carbon source with or
794 without iron and magnesium. Incubation was done at 25°C during 3 days. After this incubation
795 period, the supernatant was recovered by centrifugation (8000g, 15 min) and filtrated at 0.22µm.
796 The presence of iron chelating agents was quantified using the liquid Chromazurol assay (CAS)
797 of Schwyn and Neilands (1987). To do it, a volume of 100 µl of the supernatant inoculated or not
798 was then mixed with the CAS solution and incubated 1h at ambient temperature before reading
799 the absorbance at 655 nm with a microplate reader. Measures of control solutions at different pH
800 (*i.e.*, culture medium with adjusted from 6.5 to 2.5) permitted to confirm that the results obtained
801 in the CAS assay were not simply due to acidification only, but to the production of a chelating
802 agent by the strain PML1(12).
803
804 *RNA extraction and sequencing*

After 20h of incubation, 10 mL of culture was recovered and centrifuged at 8000 g (15 min; 4°C) to pellet the bacterial cells. Supernatants were removed and cells were frozen in liquid nitrogen and stored at - 80°C. Total RNA was purified using the RiboPure™ kit (Ambion, Austin, USA) following the manufacturer's recommendations, then treated twice with DNAse I (Ambion), precipitated with ethanol and resuspended in RNAse-free water. The concentration and quality of the extracted RNA was determined by measuring its absorbance using a Nanodrop 2000 spectrophotometer (Thermo Scientific, Waltham, MA, USA), a Qubit® RNA Assay Kit in a Qubit® 2.0 Fluorometer (Life Technologies, CA, United States) and TapeStation analyses. The RNA integrity number value was 9.0 on average. The total RNA were sent to GENEWIZ (location) which operated the rRNA depletion using the Ribo-Zero rRNA removal kit for bacteria, performed the stranded RNA library preparation and sequenced the cDNA on their Illumina HiSeq2500 platform using a 2x100bp paired-end (PE) configuration in High Output mode (V4chemistry). This sequencing generated a total of more than 250 million reads per lane.

Protein extraction and tandem mass spectrometry

After 20h of incubation, 5 mL of culture were recovered and centrifuged to pellet the bacteria. Supernatants were removed and cells were frozen in liquid nitrogen and stored at -80 °C. For each sample, the cell pellet was homogenized in a volume (25 µL per mg of cellular pellet (wet weight) of lithium dodecyl sulfate 1X lysis buffer (Invitrogen), supplemented with 200 mg of 0.1 mm silica beads (MP Biomedicals), and disrupted by bead-beating with a Precellys Evolution instrument (Bertin Technologies) operated at 7,800 rpm for 3 cycles of 20 seconds, with 30 seconds of pause between each cycle. The samples were then centrifuged at 16,000 g for 1 min. The resulting supernatants were heated at 99°C for 5 min. A volume of 25 µL of each sample was loaded on a NuPAGE 4-12% Bis-Tris gel and subjected to electrophoresis for 5 min at 200 V. After migration, the proteins were stained with Coomassie SimplyBlue SafeStain (Invitrogen). In-gel proteolysis of the whole proteome sliced in a single polyacrylamide band was performed with 0.2 µg of trypsin gold (Promega) supplemented with 50 µl of 0.01% ProteaseMAX surfactant (Promega) as previously described (Hartmann *et al*., 2014). After incubation à 37°C for 4 h, the solution was acidified with 5% trifluoroacetic acid and the final volume adjusted to 50 µl of 0.1% trifluoroacetic acid if required. A volume of 5 µl of this suspension was then injected to identify the resulting peptides by tandem mass spectrometry using a Q-Exactive HF

836 instrument (Thermo Scientific) coupled to an ultimate 300 nanoLC system (Thermo Scientific) in
837 the same conditions as those described by Hayoun (Hayoun *et al*., 2019). Peptides were resolved
838 on an Acclaim PepMap100 C18 reversed-phase column (3 µm, 100 Å, 75 µm id x 50 cm) over a
839 90 min gradient.
840
841 *Bioinformatic and statistical analyses*
842 The RNAseq reads were mapped to the coding sequences (CDS) of the genome of strain
843 PML1(12) through the Microscope (Vallenet *et al*., 2019) annotation platform using the BWA
844 (version 0.7.4-r385; Li and Durbin, 2009). Genes differentially expressed were sorted according
845 to the genome sequence of strain PML1(12)(AEJF00000000) and raw data statitics are accessible
846 on the MICROSCOPE platform (https://mage.genoscope.cns.fr/microscope/home/index.php?
847 act=logout; login: guest2020 password: Ic7Hf3). Raw data are under deposit on EMB-EBI
848 (https://www.ebi.ac.uk/arrayexpress/; E_N00000). For proteins, MS/MS spectra were queried
849 against a database with the theoretical coding sequences of *Caballeronia mineralivorans*
850 PML1(12) using the Mascot Daemon software version 2.6.1 (Matrix Science). The parameters
851 used for this search were: peptide charge of 2+ or 3+, 5 ppm peptide tolerance, 0.02 Da MS/MS
852 fragment tolerance, carbamidomethylation of cysteine as fixed modification, and oxidation of
853 methionine as variable modification. A protein was validated on the basis of two identified
854 peptide sequences and with a final discovery rate of less than 1% as estimated with a decoy
855 database search. Proteins differentially produced were also sorted according to the genome
856 sequence of strain PML1(12) and a matrix generated (Pride access n° PXD000000). The effect of
857 the different treatments (*i.e.,* GB, GBwB and MBwB) on both RNA and protein datasets was
858 determined using the Mixomics R package (González *et al*., 2012; Rohart *et al*., 2017). To do it,
859 the full raw dataset of each approach (i.e., RNA or protein) was first normalized to conserve the
860 genes which abundance presented a minimum of 100 in the RNAseq dataset in one the treatments
861 considered and a minimum 30 in the proteome dataset. A partial Least Squares (PLS) regression
862 was first done to integrate the RNAseq and proteome matrix to generate a global view. Due to the
863 complexity of our dataset and to allow interpretability a Sparse Partial Least Squares regression
864 (sPLS) was then performed as it permits to perform simultaneous variable selection in the two
865 data sets. The dimensions selected were determined based on the higher variance explained and
866 the number of variables (*i.e.,* genes) considered in the sPLS were limited to 100 per component

axis and method (transcriptomics or proteomics) for legibility and interpretability reasons. The distribution of the different genes considered was then visualized in a correlation circle plot permitting to evidence treatment specific genes. The list of genes was then compared to the outputs of the DESeq2 analysis. The DESeq2 (Anders and Huber, 2010; Love *et al*., 2014) was used to calculate differential gene expression and protein abundance between the different treatments. A normalization of read numbers for replicates in each treatment was performed (by estimates of size factors in DESeq2 and normalization), then differential expression values (FoldChange) and statistical values (pVal and adjusted pVal through the Benjamini and Hochberg's approaches) assessing the false discovery rate (FDR) were calculated. All genes having an adjusted p-value inferior to 0.05 and a cut-off for absolute fold change > 1 were considered as significantly differentially expressed. For the proteomics data, a cut-off for fold change > 0.3 was considered.

Concerning the chemical analyses, the effect of the different treatments on the organic acid production, the pH and inorganic nutrients released in solution was determined by analysis of variance (one way ANOVA, $p < 0.05$, followed by a Tukey test).

ACKNOWLEDGEMENTS

This work was supported by grants from the EC2CO program of the CNRS and the Labex ARBRE from the French National Research Agency (ANR) to S.U. The UMR1136 and UR1138 are supported by the ANR through the Labex Arbre (ANR-11-LABX-0002-01). L.P. is supported by a PhD fellowship from the French Ministère de l'Enseignement Supérieur, de la Recherche et de l'Innovation. The authors thank : Dr. P. Frey-Klett for helpful discussions, C. Cochet for the geochemical analyses, E. Morin for bioinformatics and statistical supports; the MICROSCOPE team (David Roche; Genoscope) for the support provided on the genome and transcriptome management.

REFERENCES

Ahmed, E., and Holmström, S. J. (2014). Siderophores in environmental research: roles and applications. Microbial Biotechnology, 7(3), 196-208.

An, R., and Moe, L. A. (2016). Regulation of PQQ-dependent glucose dehydrogenase activity in the model rhizosphere dwelling bacterium *Pseudomonas putida* KT2440. Applied and Environmental Microbiology, 82(16), 4955-4964.

Anders S, Huber W. Differential expression analysis for sequence count data. Genome Biol. 2010;11:R106.

Andrews, S.C., Robinson, A.K., and Rodríguez-Quiñones, F. (2003). Bacterial iron homeostasis. FEMS Microbiology Reviews, 27(2-3), 215-237.

April, R., and Newton, R. (1992). Mineralogy and mineral weathering. In Atmospheric deposition and forest nutrient cycling (pp. 378-425). Springer, New York, NY.

Argüelles, J.C. (2000). Physiological roles of trehalose in bacteria and yeasts: a comparative analysis. Archives of Microbiology, 174(4), 217-224.

Babu-Khan, S., Yeo, T. C., Martin, W. L., Duron, M. R., Rogers, R. D., and Goldstein, A. H. (1995). Cloning of a mineral phosphate-solubilizing gene from *Pseudomonas cepacia*. Appl. Environ. Microbiol., 61(3), 972-978.

Balland, C., Poszwa, A., Leyval, C., and Mustin, C. (2010). Dissolution rates of phyllosilicates as a function of bacterial metabolic diversity. Geochimica et Cosmochimica Acta, 74(19), 5478-5493.

Banfield, J. F., and Nealson, K. H. (Eds.). (2018). Geomicrobiology: Interactions between microbes and minerals (Vol. 35). Walter de Gruyter GmbH and Co KG. Washington DC, USA.

Brantley, S. L. (2008). Kinetics of mineral dissolution. In Kinetics of water-rock interaction (pp. 151-210). Springer, New York, NY.

Bryce, C. C., Le Bihan, T., Martin, S. F., Harrison, J. P., Bush, T., Spears, B., ... and Cockell, C. S. (2016). Rock geochemistry induces stress and starvation responses in the bacterial proteome. Environmental Microbiology, 18(4), 1110-1121.

Buch A, Archana G, Naresh Kumar G (2008) Metabolic channeling of glucose towards gluconate in phosphate-solubilizing *Pseudomonas aeruginosa* P4 under phosphorus deficiency. Research in Microbiology, 159(9):635–642.

Cai, X., Huang, L., Yang, G., Yu, Z., Wen, J., and Zhou, S. (2018). Transcriptomics, proteomics and bioelectrochemical characterization of an exoelectrogen *Geobacter soli* grown with different electron acceptors. Frontiers in Microbiology, 9, 1075.

926 Calvaruso, C., Turpault, M. P., and Frey-Klett, P. (2006). Root-associated bacteria contribute to
927 mineral weathering and to mineral nutrition in trees: a budgeting analysis. Applied and
928 Environmental Microbiology, 72(2), 1258-1266.
929 Calvaruso, C., Turpault, M. P., Frey-Klett, P., Uroz, S., Pierret, M. C., Tosheva, Z., and Kies, A.
930 (2013). Increase of apatite dissolution rate by Scots pine roots associated or not with
931 *Burkholderia glathei* PML1(12)Rp in open-system flow microcosms. Geochimica et
932 Cosmochimica Acta, 106, 287-306.
933 Carmichael, J. R., Zhou, H., and Butler, A. (2019). A suite of asymmetric citrate siderophores
934 isolated from a marine *Shewanella* species. Journal of Inorganic Biochemistry, 198, 110736.
935 Carroll, C. S., and Moore, M. M. (2018). Ironing out siderophore biosynthesis: a review of non-
936 ribosomal peptide synthetase (NRPS)-independent siderophore synthetases. Critical Reviews in
937 Biochemistry and Molecular Biology, 53(4), 356-381.
938 Cavener DR. 1992. GMC oxidoreductases. Journal of Molecular Biology, 223:811–814.
939 Challis, G. L. (2005). A widely distributed bacterial pathway for siderophore biosynthesis
940 independent of nonribosomal peptide synthetases. ChemBioChem, 6(4), 601-611.
941 Childers, S. E., Ciufo, S., and Lovley, D. R. (2002). *Geobacter metallireducens* accesses
942 insoluble Fe (III) oxide by chemotaxis. Nature, 416(6882), 767-769.
943 Colin, Y., Nicolitch, O., Turpault, M. P., and Uroz, S. (2017). Mineral types and tree species
944 determine the functional and taxonomic structures of forest soil bacterial communities. Applied
945 and Environmental Microbiology, 83(5), e02684-16.
946 Drever, J. I. (1994). The effect of land plants on weathering rates of silicate minerals.
947 Geochimica et Cosmochimica Acta, 58(10), 2325-2332.
948 Goldstein, A. H. (1995). Recent progress in understanding the molecular genetics and
949 biochemistry of calcium phosphate solubilization by gram negative bacteria. Biological
950 Agriculture and Horticulture, 12(2), 185-193.
951 González, I., Lê Cao, K. A., Davis, M. J., and Déjean, S. (2012). Visualising associations
952 between paired 'omics' data sets. BioData mining, 5(1), 19.
953 Gyaneshwar P, Parekh L, Archana G, Poole P, Collins M, Hutson R, Kumar GN. 1999.
954 Involvement of a phosphate starvation inducible glucose dehydrogenase in soil phosphate
955 solubilization by *Enterobacter asburiae*. FEMS Microbiology Letters, 171: 223-229.

Hartmann, E. M., Allain, F., Gaillard, J. C., Pible, O., and Armengaud, J. (2014). Taking the shortcut for high-throughput shotgun proteomic analysis of bacteria. In Host-Bacteria Interactions (pp. 275-285). Humana Press, New York, NY.

Hayoun, K., Gouveia, D. D., Grenga, L., Pible, O., and Armengaud, J. (2019). Evaluation of sample preparation methods for fast proteotyping of microorganisms by tandem mass spectrometry. Frontiers in microbiology, 10, 1985.

Huang, J., Sheng, X. F., Xi, J., He, L. Y., Huang, Z., Wang, Q., and Zhang, Z. D. (2014). Depth-related changes in community structure of culturable mineral weathering bacteria and in weathering patterns caused by them along two contrasting soil profiles. Applied and Environmental Microbiology, 80(1), 29-42.

Hutchens, E. (2009). Microbial selectivity on mineral surfaces: possible implications for weathering processes. Fungal Biology Reviews, 23(4), 115-121.

Ishige, T., Krause, M., Bott, M., Wendisch, V. F., and Sahm, H. (2003). The phosphate starvation stimulon of *Corynebacterium glutamicum* determined by DNA microarray analyses. Journal of Bacteriology, 185(15), 4519-4529.

Jolivet, C., Angers, D. A., Chantigny, M. H., Andreux, F., and Arrouays, D. (2006). Carbohydrate dynamics in particle-size fractions of sandy spodosols following forest conversion to maize cropping. Soil Biology and Biochemistry, 38(9), 2834-2842.

Koele, N., Turpault, M. P., Hildebrand, E. E., Uroz, S., and Frey-Klett, P. (2009). Interactions between mycorrhizal fungi and mycorrhizosphere bacteria during mineral weathering: budget analysis and bacterial quantification. Soil Biology and Biochemistry, 41(9), 1935-1942.

Landeweert, R., Hoffland, E., Finlay, R. D., Kuyper, T. W., and van Breemen, N. (2001). Linking plants to rocks: ectomycorrhizal fungi mobilize nutrients from minerals. Trends in Ecology and Evolution, 16(5), 248-254.

Li, H., and Durbin, R. (2009). Fast and accurate short read alignment with Burrows–Wheeler transform. Bioinformatics, 25(14), 1754-1760.

Liermann, L. J., Kalinowski, B. E., Brantley, S. L., and Ferry, J. G. (2000). Role of bacterial siderophores in dissolution of hornblende. Geochimica et Cosmochimica Acta, 64(4), 587-602.

Lepleux, C., Uroz, S., Collignon, C., Churin, J. L., Turpault, M. P., and Frey-Klett, P. (2013). A short-term mineral amendment impacts the mineral weathering bacterial communities in an acidic forest soil. Research in Microbiology, 164(7), 729-739.

Lim, C. K., Hassan, K. A., Tetu, S. G., Loper, J. E., and Paulsen, I. T. (2012). The effect of iron limitation on the transcriptome and proteome of *Pseudomonas fluorescens* Pf-5. PloS one, 7(6), e39139.

de Lorenzo, V., Bindereif, A., Paw, B.H., and Neilands, J. B. (1986). Aerobactin biosynthesis and transport genes of plasmid ColV-K30 in *Escherichia coli* K-12. Journal of Bacteriology, 165(2), 570-578.

Love, M. I., Huber, W., and Anders, S. (2014). Moderated estimation of fold change and dispersion for RNA-seq data with DESeq2. Genome Biology, 15(12), 550.

Lynch, D., O'Brien, J., Welch, T., Clarke, P., ÓCuív, P., Crosa, J. H., and O'Connell, M. (2001). Genetic organization of the region encoding regulation, biosynthesis, and transport of rhizobactin 1021, a siderophore produced by *Sinorhizobium meliloti*. Journal of Bacteriology, 183(8), 2576-2585.

Mailloux, B. J., Alexandrova, E., Keimowitz, A. R., Wovkulich, K., Freyer, G. A., Herron, M., Stolz JF, Kenna TC, Pichler T, Polizzotto ML, Dong H, Bishop M, Knappett PS. (2009). Microbial mineral weathering for nutrient acquisition releases arsenic. Applied and Environmental Microbiology, 75(8), 2558-2565.

Mander C, Wakelin S, Young S, Condron L, O'Callaghan M. 2012. Incidence and diversity of phosphate-solubilising bacteria are linked to phosphorus status in grassland soils. Soil Biology and Biochemistry, 44: 93-101.

Mapelli, F., Marasco, R., Balloi, A., Rolli, E., Cappitelli, F., Daffonchio, D., and Borin, S. (2012). Mineral–microbe interactions: biotechnological potential of bioweathering. Journal of Biotechnology, 157(4), 473-481.

Medeiros, P. M., Fernandes, M. F., Dick, R. P., and Simoneit, B. R. (2006). Seasonal variations in sugar contents and microbial community in a ryegrass soil. Chemosphere, 65(5), 832-839.

Nicolitch, O., Colin, Y., Turpault, M. P., and Uroz, S. (2016). Soil type determines the distribution of nutrient mobilizing bacterial communities in the rhizosphere of beech trees. Soil Biology and Biochemistry, 103, 429-445.

Nicolitch, O., Feucherolles, M., Churin, J. L., Fauchery, L., Turpault, M. P., and Uroz, S. (2019). A microcosm approach highlights the response of soil mineral weathering bacterial communities to an increase of K and Mg availability. Scientific Reports, 9(1), 14403.

Olsson-Francis, K., Van Houdt, R., Mergeay, M., Leys, N., and Cockell, C.S. (2010). Microarray analysis of a microbe–mineral interaction. Geobiology, 8(5), 446-456.

Or, D., Smets, B. F., Wraith, J. M., Dechesne, A., and Friedman, S. P. (2007). Physical constraints affecting bacterial habitats and activity in unsaturated porous media–a review. Advances in Water Resources, 30(6-7), 1505-1527.

Picard L., Turpault, M-P., Oger, P., Uroz, S. A FAD-dependent glucose dehydrogenase confers its mineral weathering ability to *Collimonas pratensis* PMB3(1). Submitted (need to add journal).

Preiss, J., and Romeo, T. (1994). Molecular biology and regulatory aspects of glycogen biosynthesis in bacteria. Progress in Nucleic Acid Research and Molecular Biology, 47:329-399.

Rohart, F., Gautier, B., Singh, A., & Lê Cao, K. A. (2017). mixOmics: An R package for 'omics feature selection and multiple data integration. PLoS Computational Biology, 13(11), e1005752.

Sasnow, S. S., Wei, H., and Aristilde, L. (2016). Bypasses in intracellular glucose metabolism in iron-limited *Pseudomonas putida*. MicrobiologyOpen, 5(1), 3-20.

Schwyn, B., and Neilands, J. B. (1987). Universal chemical assay for the detection and determination of siderophores. Analytical Biochemistry, 160(1), 47-56.

Sützl, L., Foley, G., Gillam, E.M.J., Bodén, M., Haltrich, D. (2019). The GMC superfamily of oxidoreductases revisited: analysis and evolution of fungal GMC oxidoreductases. Biotechnology and Biofuels 12,1–18.

Sun, Q., Fu, Z., Finlay, R., and Lian, B. (2019). Transcriptome analysis provides novel insights into the capacity of the ectomycorrhizal fungus *Amanita pantherina* to weather K-containing feldspar and apatite. Applied and Environmental Microbiology, 85(15), e00719-19.

Uroz, S., Calvaruso, C., Turpault, M. P., Pierrat, J. C., Mustin, C., and Frey-Klett, P. (2007). Effect of the mycorrhizosphere on the genotypic and metabolic diversity of the bacterial communities involved in mineral weathering in a forest soil. Applied and Environmental Microbiology, 73(9), 3019-3027.

Uroz, S., Calvaruso, C., Turpault, M. P., and Frey-Klett, P. (2009). Mineral weathering by bacteria: ecology, actors and mechanisms. Trends in Microbiology, 17(8), 378-387.

Uroz, S., Turpault, M. P., Van Scholl, L., Palin, B., and Frey-Klett, P. (2011). Long term impact of mineral amendment on the distribution of the mineral weathering associated bacterial communities from the beech *Scleroderma citrinum* ectomycorrhizosphere. Soil Biology and Biochemistry, 43(11), 2275-2282.

1048 Uroz, S., Kelly, L. C., Turpault, M. P., Lepleux, C., and Frey-Klett, P. (2015). The
1049 mineralosphere concept: mineralogical control of the distribution and function of mineral-
1050 associated bacterial communities. Trends in Microbiology, 23(12), 751-762.
1051 Uroz, S., and Oger, P. (2015). Draft genome sequence of *Burkholderia* sp. strain PML1 (12), an
1052 ectomycorrhizosphere-inhabiting bacterium with effective mineral-weathering ability. Genome
1053 Announcements, 3(4), e00798-15.
1054 Uroz, S., and Oger, P. (2017). *Caballeronia mineralivorans* sp. nov., isolated from oak-
1055 *Scleroderma citrinum* mycorrhizosphere. Systematic and Applied Microbiology, 40(6), 345-351.
1056 Vallenet, D., Belda, E., Calteau, A., Cruveiller, S., Engelen, S., Lajus, A., et al (2012).
1057 MicroScope—an integrated microbial resource for the curation and comparative analysis of
1058 genomic and metabolic data. Nucleic Acids Research, 41(D1), D636-D647.
1059 Vallenet, D., Calteau, A., Mathieu Dubois, M., Amours, P., Bazin, A., Beuvin, M., Burlot, L.,
1060 Bussell, X., Fouteau, S., Gautreau, G., Lajus, A., Langlois, J., Planel, R., Roche, D., Rollin, J.,
1061 Rouy, Z., Sabatet, V., Médigue, C. (2019) MicroScope: an integrated platform for the annotation
1062 and exploration of microbial gene functions through genomic, pangenomic and metabolic
1063 comparative analysis. Nucleic Acids Research. 48(D1), D579-D589.
1064 Vieira, S., Sikorski, J., Gebala, A., Boeddinghaus, R. S., Marhan, S., Rennert, T., et al (2020).
1065 Bacterial colonization of minerals in grassland soils is selective and highly dynamic.
1066 Environmental Microbiology, 22(3), 917-933.
1067 Wadhams, G. H., and Armitage, J. P. (2004). Making sense of it all: bacterial chemotaxis. Nature
1068 reviews Molecular Cell Biology, 5(12), 1024-1037.
1069 Wang, Q., Cheng, C., He, L., Huang, Z., and Sheng, X. (2014). Characterization of depth-related
1070 changes in bacterial communities involved in mineral weathering along a mineral-rich soil
1071 profile. Geomicrobiology Journal, 31(5), 431-444.
1072 Wang, W., Lian, B., and Pan, L. (2015). An RNA-sequencing study of the genes and metabolic
1073 pathways involved in *Aspergillus niger* weathering of potassium feldspar. Geomicrobiology
1074 Journal, 32(8), 689-700.
1075 Wang, Y. L., Sun, L. J., Xian, C. M., Kou, F. L., Zhu, Y., He, L. Y., and Sheng, X. F. (2020).
1076 Interactions between Biotite and the Mineral-Weathering Bacterium *Pseudomonas azotoformans*
1077 F77. Applied and Environmental Microbiology, 86(7).

1078 Xiao, B., Lian, B., and Shao, W. (2012). Do bacterial secreted proteins play a role in the
1079 weathering of potassium-bearing rock powder? Geomicrobiology Journal, 29(6), 497-505.
1080 Yamaoka H, Yamashita Y, Ferri S, Sode K. 2008. Site directed mutagenesis studies of FAD-
1081 dependent glucose dehydrogenase catalytic subunit of *Burkholderia cepacia*. Biotechnology
1082 Letters 30:1967–1972.
1083 Yee, N., Fein, J. B., and Daughney, C. J. (2000). Experimental study of the pH, ionic strength,
1084 and reversibility behavior of bacteria–mineral adsorption. Geochimica et Cosmochimica Acta,
1085 64(4), 609-617.
1086 Zeng, Q., Wu, X., and Wen, X. (2016). Effects of soluble phosphate on phosphate-solubilizing
1087 characteristics and expression of *gcd* gene in *Pseudomonas frederiksbergensis* JW-SD2. Current
1088 Microbiology, 72(2), 198-206.

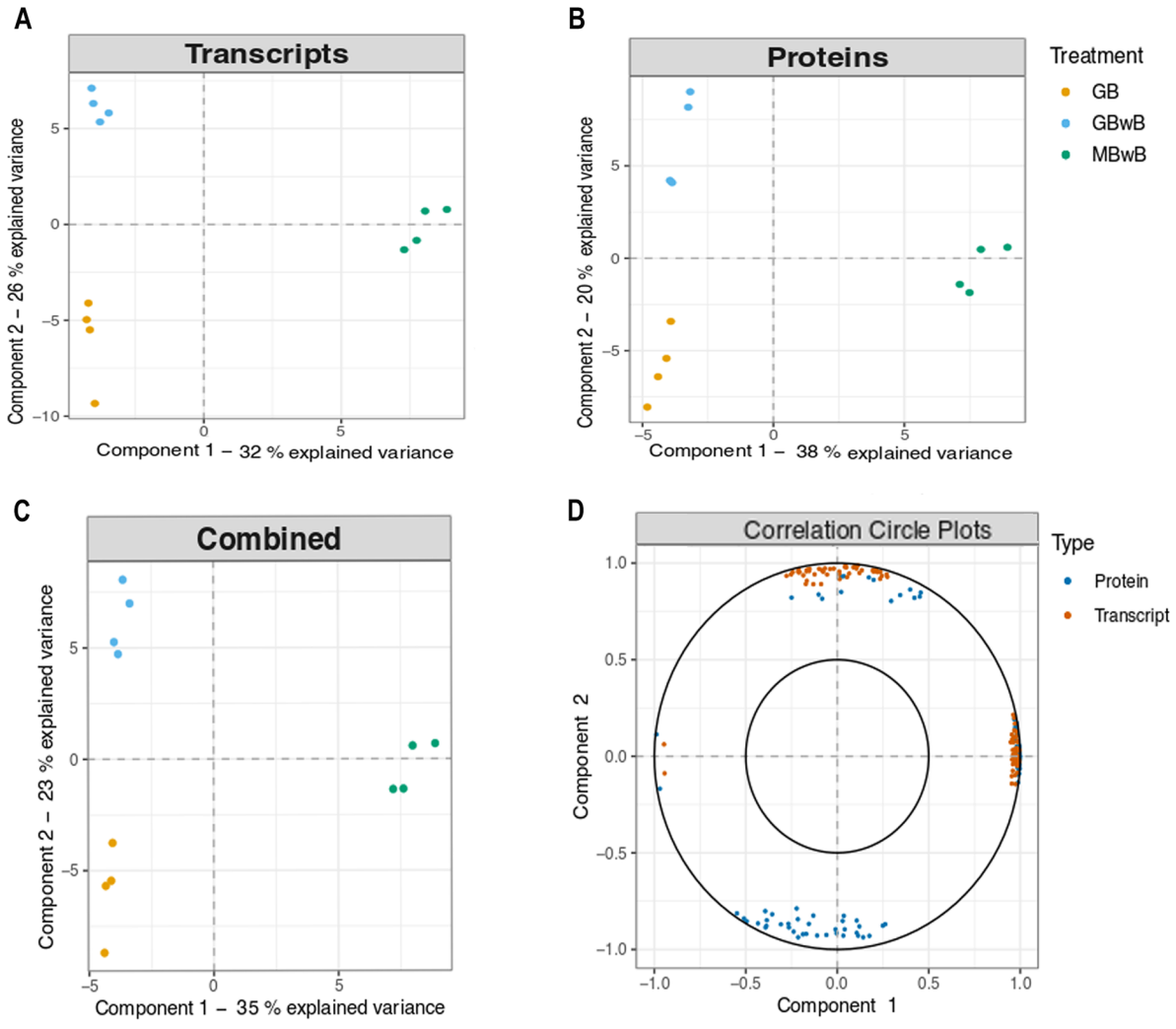
A
Transcripts
Component 2 – 26 % explained variance
Component 1 – 32 % explained variance
B
Proteins
Component 2 – 20 % explained variance
Component 1 – 38 % explained variance
Treatment
GB
GBwB
MBwB
C
Combined
Component 2 – 23 % explained variance
Component 1 – 35 % explained variance
D
Correlation Circle Plots
Component 2
Component 1
Type
Protein
Transcript

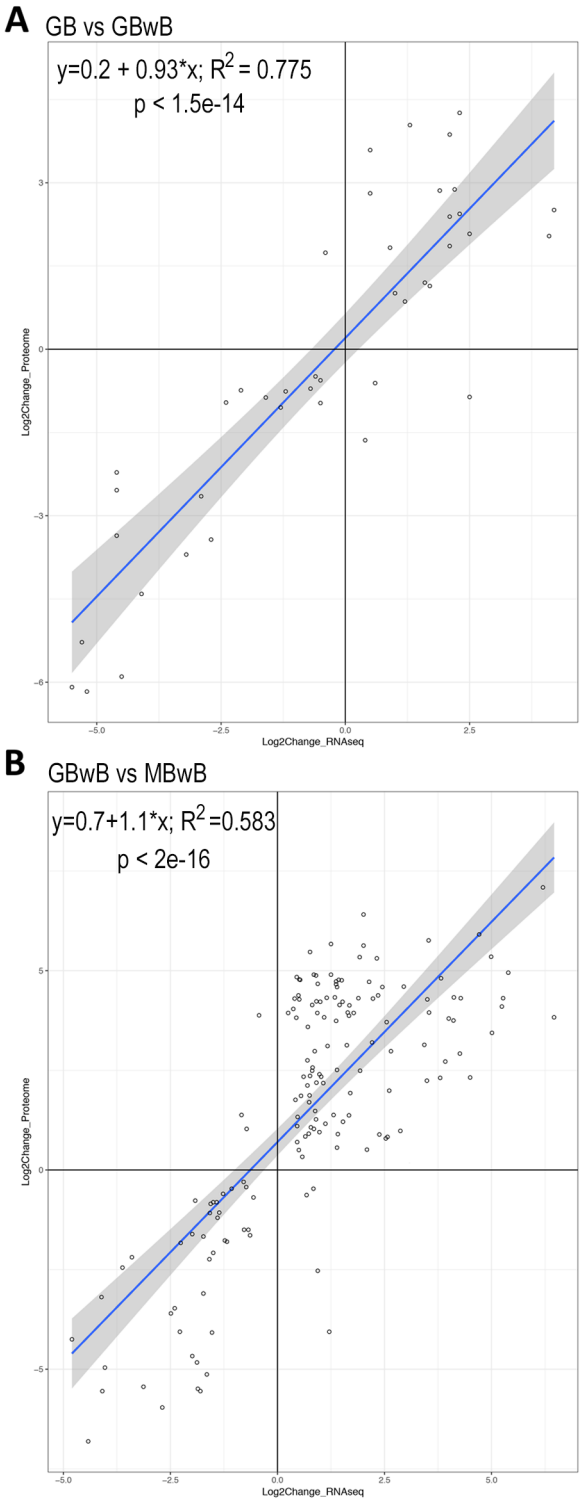
A
GB vs GBwB
y=0.2 + 0.93*x; R2 = 0.775
p < 1.5e-14
Log2Change_Proteome
Log2Change_RNAseq
B
GBwB vs MBwB
y=0.7+1.1*x; R2 =0.583
p < 2e-16
Log2Change_Proteome
Log2Change_RNAseq

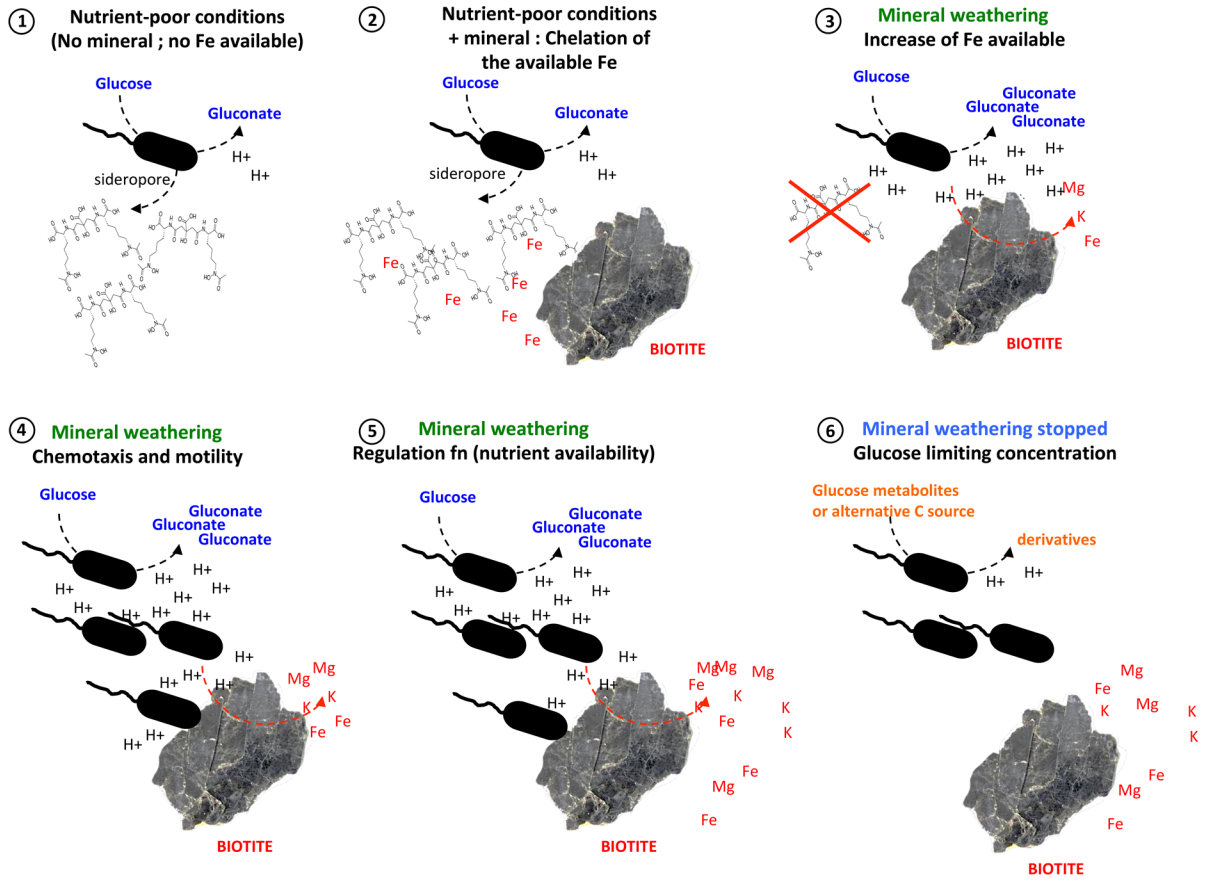
1
Nutrient-poor conditions
(No mineral ; no Fe available)
Glucose
Gluconate
H+
sideropore
2
Nutrient-poor conditions
+ mineral : Chelation of
the available Fe
Glucose
Gluconate
sideropore
Fe
BIOTITE
3
Mineral weathering
Increase of Fe available
Glucose
Gluconate
Mg
K
Fe
BIOTITE
4
Mineral weathering
Chemotaxis and motility
Glucose
Gluconate
Mg
K
Fe
BIOTITE
5
Mineral weathering
Regulation fn (nutrient availability)
Glucose
Gluconate
Mg
Fe
K
BIOTITE
6
Mineral weathering stopped
Glucose limiting concentration
Glucose metabolites
or alternative C source
derivatives
Mg
Fe
K
BIOTITE